

Machine Learning for Sensor Transducer Conversion Routines

Thomas Newton, James T. Meech, *Student Member, IEEE* and Phillip Stanley Marbell, *Senior Member, IEEE*

Abstract—Sensors with digital outputs require software conversion routines to transform the unitless ADC samples to physical quantities with the correct units. These conversion routines are computationally complex given the limited computational resources of low-power embedded systems. This article presents a set of machine learning methods to learn new, less-complex conversion routines that do not sacrifice accuracy for the BME680 environmental sensor. We present a Pareto analysis of the tradeoff between accuracy and computational overhead for the models and present models that reduce the computational overhead of the existing industry-standard conversion routines for temperature, pressure, and humidity by 62%, 71%, and 18% respectively. The corresponding RMS errors for these methods are 0.0114 °C, 0.0280 KPa, and 0.0337%. These results show that machine learning methods for learning conversion routines can produce conversion routines with reduced computational overhead while maintaining good accuracy.

Index Terms—Machine Learning, Regression, Sensor.

I. INTRODUCTION

THERE is a constant drive to make sensors smaller and more power-efficient. Users require embedded sensor systems such as wearable fitness trackers and battery-powered smart thermostats to be small with long battery life. In resource-constrained sensor applications, engineers optimize code for a small memory footprint and low computational overhead [1].

This article describes new methods to optimise the computational overhead of the conversion routines for the BME680, a digital temperature, pressure, humidity, and indoor air quality sensor [2]. Conversion routines are essential for digital sensors to have meaningful outputs. Embedded sensor systems require low-power microcontrollers with sufficient random-access memory (RAM), flash storage, and computational performance to store and run the conversion routines to make use of sensors: Optimising the conversion routines will help meet these requirements under tighter memory size and power consumption constraints.

A. Contributions

This article makes the following three contributions. The article presents:

- 1) A new approach and its implementation of alternative, machine-learned conversion routines for temperature, pressure, and humidity measurements. We demonstrate the methods using a state-of-the-art sensor, the Bosch

Thomas Newton, James T. Meech and Phillip Stanley Marbell are with the Department of Engineering, University of Cambridge, Cambridge, UK CB3 0FF e-mail: phillip.stanley-marbell@eng.cam.ac.uk.

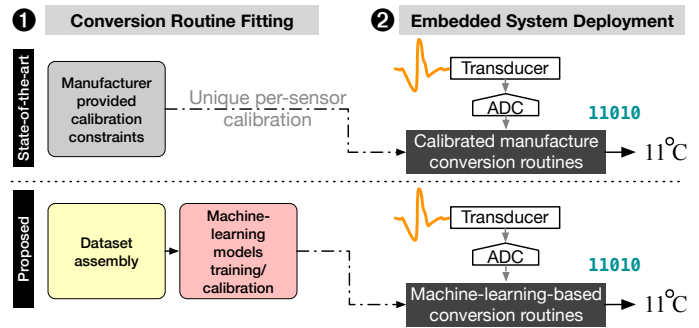


Fig. 1. Block diagrams for the original and the new learned conversion routines. The values shown are for the temperature conversion on the BME680 sensor [2].

BME680 but the insights and methods could be applied to other sensors.

- 2) Quantitative evaluation of the computational overhead, accuracy, RAM, and flash storage usage of these conversion routines.
- 3) A Pareto analysis of accuracy against computational overhead for the conversion routines.

B. Why do Sensors Need Conversion Routines?

Typical sensors with digital outputs have a transducer which is sensitive to the signal they are designed to measure (the measurand), e.g., temperature, and produce a voltage which is converted to a digital signal by an analogue-to-digital converter (ADC). The ADC outputs a single unsigned integer with a fixed number of bits (the measurement). Obtaining a reading with meaningful units requires a transformation to map these unsigned integers into the correct real number range. If the transducer is non-linear then the conversion must also invert the transfer function of the transducer.

C. Manufacturer-Provided Conversion Routines

The top half of Figure 1 shows a block diagram for the BME680 conversions provided by Bosch Sensortec [2]. An external microcontroller computes the conversion routines in real time each time the microcontroller samples the sensor. For the BME680, the manufacturer provides calibration constants specific to each individual sensor. These are parameters of the conversion routine, which tune the conversion on a per-sensor basis to reduce the impact of any manufacturing variability in sensor properties.

D. Learning New Conversions from Data

We can use machine learning methods to learn alternative conversion routines from data. The bottom half of Figure 1 shows a block diagram of the process. Using the original manufacturer-provided conversion routines and a set of calibration constants, our method generates training datasets, to train the models. Our method saves the trained weights so that at inference time the models are a direct replacement for the manufacturer-provided conversion routines in Figure 1. The calibration constants used to generate the training data are specific to one physical sensor, therefore the trained weights will only be accurate for that sensor.

II. TRAINING DATA

We produced synthetic mesh datasets and sequence datasets for training and testing the models. The synthetic datasets take the original conversion routines, provided by the manufacturer [2], as ground truth. We generated mesh datasets by producing a fine mesh of equally-spaced points across the unconverted domain. We applied the original conversion routines to produce labels for all of these data points.

To produce datasets which are continuous sequences, we used Gaussian processes, adjusting the characteristics using a kernel function. We used a five-halves Matern kernel function and set the length scale to 20 times the virtual sampling period. The virtual sampling period is the constant interval between evaluating the Gaussian process and has no link to any real sampling period. To ensure that the generated sequence fills the required range, we apply a linear transformation after generating the function. This makes the amplitude parameter of the kernel function irrelevant. For multi-dimensional inputs, we evaluated a single dimensional sample function for each input. We drew sample functions independently from the same single dimensional Gaussian process. We applied the original conversions to provide labels for the dataset.

An optional refinement, we call the inverse refinement, ensures datasets precisely match the operating range of the sensor. Instead of generating data in the unconverted domain, we generate data in the converted domain, where it is easy to enforce the limits of the specified operating range. We compute the unconverted values by inverting the original conversion routines.

III. EVALUATION METHOD

We measured the accuracy of the models using a sequence of synthetic data which was 1000 points long. We averaged each result over ten similar datasets. For models that included an element of randomness such as neural networks, we averaged the results over five different random seeds.

A. Accuracy Measure

Let y_{Predict} be the value predicted by the machine learning model, y_{True} be the ground truth value from the original conversion routine, and $y_{\text{True}}^{(\text{Max})}$ and $y_{\text{True}}^{(\text{Min})}$ be the maximum and minimum values of the operating range of the sensor for

the physical quantity of interest. We used a normalised RMS error to quantify accuracy, where:

$$E_{\text{RMS}} = \sqrt{\sum_i \left((y_{\text{Predict}}^{(i)} - y_{\text{True}}^{(i)}) \times \frac{100}{y_{\text{True}}^{(\text{Max})} - y_{\text{True}}^{(\text{Min})}} \right)^2}. \quad (1)$$

This allows for comparison between the measurements from different sensors (e.g., pressure measurements with a range of 80 kPa and humidity measurements with a range of 100%).

B. Computational Overhead and Memory Usage Measures

We first implemented each model in Python making use of the TensorFlow library [3]. We then exported the trained weights and created C-language implementations of the inference functions based on these weights. We measured overhead as the number of RISC-V instructions needed to convert a single ADC sample into a physically-meaningful real-valued number with units. We used the Sunflower embedded system emulator [4] to measure the number of dynamic instructions executed at run time by a binary compiled from a given C-language implementation: We used a feature in Sunflower to precisely and deterministically measure the dynamic instructions executed for a given region of source code. We measured the flash and RAM usage of the implementations of the models generated by each machine learning method by taking the size of the `.text` section as the flash storage requirement. We summed the `.bss` and `.data` section sizes to determine the RAM requirement for global variables and manually counted the memory required for local variables.

IV. TESTED MODELS

We evaluated both function approximation methods as well as time series methods.

A. Function Approximation Methods

We trained most models with datasets generated by the mesh method described in Section II using the inverse refinement and 20 discretisation levels each for temperature, pressure, and humidity. We used other datasets where explicitly mentioned. The methods that we trained fall into five broad categories:

1) *Linear Regression*: Simple linear-in-the-parameters regression using linear feature vectors. We used a simple non-Bayesian linear regression.

2) *Quadratic Regression*: A linear-in-the-parameters regression using quadratic feature vectors.

3) *Linear Interpolation Lookup Table*: A lookup table that linearly interpolates between three nearby points in the lookup table. We used bespoke datasets using the mesh method described in Section II without the inverse refinement. We did this to ensure a regular, square grid in the unconverted (input) domain to simplify the interpolation. We tested discretisation levels of 3, 10, and 20.

4) *Gaussian Process Regression*: Gaussian Process regression as described by Rasmussen [5]. We used a Gaussian likelihood function and Gaussian kernel to solve the regression analytically. The training datasets used discretisation levels of two and three. We optimised the hyper-parameters in the kernel function to maximise the log-likelihood of generating the data.

5) *Neural Networks*: Simple feed-forward fully-connected neural networks. Every neuron uses the same activation function. A preliminary evaluation showed that the exponential, Gaussian kernel, sigmoid, RELU, hard sigmoid, tanh, and soft sign activation functions had dynamic instruction overheads of 109, 131, 122, 19, 33, 124, and 11 RISC-V instructions respectively. We therefore chose to use the RELU function because it is commonly used and has low computational overhead (19 dynamic instructions). We trained models to minimise the RMS error (Equation 1). To aid training, we rescaled the inputs and outputs to the range $[0, 1]$.

B. Sequence-Based Models

Sequence-based models may be able to provide lower computational overhead by taking advantage of the fact that the sensors measure physical systems and we have prior knowledge of what a sequence of sensor data might look like.

We trained all the sequence-based models to minimise the RMS error. We generated training datasets 5000 points long using the sequence method from Section II. Training required approximately 20000 epochs. By comparison, the feed-forward neural networks required fewer than 10000 epochs. The sequence-based models we trained fall into four broad categories:

1) *Auto-Regressive Moving Average (ARMA)*: ARMA models are usually used in systems with many wide sense stationarity assumptions and where the inputs are white noise. With these assumptions the optimal parameters can be computed analytically but in this case, with no simplifying assumptions, we trained them iteratively using TensorFlow.

2) *Gated Recurrent Unit (GRU)*: A single GRU cell with a history vector of length one, providing a scalar output as required. There are two slightly different versions of the GRU: We used the version proposed by Chung et al. [6], but both usually perform similarly [6]. Long short term memory (LSTM) neurons, used by Oldfrey et al. [7] are more complicated than the GRU so they will have higher computational overhead.

3) *Half GRU*: A GRU cell without the output gate. The output is returned directly after applying the activation function. This serves to reduce computational overhead compared to the normal GRU.

4) *Simple RNN*: The simple RNN is the least-complex of all, with no gating. The non-linear activation function allows it to model more complex data than the ARMA models.

V. EXPERIMENTAL EVALUATION

Temperature conversion routines: Figure 2(a) shows the Pareto plot of error and computational overhead for the temperature conversion routine. Quadratic regression (\clubsuit) Pareto dominates the original conversion (its normalised RMS error was of the order 10^{-12} , rounded to 0) and its computational overhead is 47% lower than the original. Linear regression ($\color{orange}{\clubsuit}$) achieves a 62% reduction in overhead compared to the original. There is a small increase in normalised RMS error, from approximately 10^{-12} to 0.00909, which corresponds to an RMS error of 0.0114°C . Figure 3(a) shows that the linear

and quadratic regression also have lower RAM and flash storage usage than any of the other methods including the original.

Pressure conversion routines: Figure 2(b) shows that the pressure Pareto frontier includes the original ($\color{blue}{\clubsuit}$), the linear interpolation lookup table with 400 entries ($\color{green}{\star}$), the quadratic regression (\clubsuit), and the linear regression ($\color{orange}{\clubsuit}$). The original conversion has zero error by definition since we used it as ground truth. The linear interpolation lookup table with 400 entries ($\color{green}{\star}$) has the next smallest error of 0.0223 with an overhead reduction of 49%. Although it results in an increase in normalised error of 0.0350 (i.e., 28.0 Pa), quadratic regression (\clubsuit) offers a larger reduction in computational overhead of 71% compared to the original. Linear regression ($\color{orange}{\clubsuit}$) offers a greater reduction in overhead of 85% but with increased error of up to 0.998 which is 798 Pa. Figure 3(b) shows that the linear and quadratic regression have lower resource usage than the original but the linear interpolation lookup table with 400 entries ($\color{green}{\star}$) has a high RAM usage of 1652 bytes compared to 60 bytes for the original conversion routine. This is because it stores a lookup table consisting of 400 floating-point numbers in RAM. Storing the lookup table in flash storage would be possible but it would increase the overhead due to the need to move the data between flash storage and memory.

Humidity conversion routines: Figure 2(c) shows the Pareto plot for the humidity conversion. The Pareto frontier includes the same four methods as for the pressure: original ($\color{blue}{\clubsuit}$), the linear interpolation lookup table with 400 entries ($\color{green}{\star}$), quadratic (\clubsuit) and linear ($\color{orange}{\clubsuit}$) regression. As before the original conversion ($\color{blue}{\clubsuit}$) has an error of 0. The linear interpolation lookup table with 400 entries ($\color{green}{\star}$) has normalised error of 0.0344 and an overhead reduction of 18%. Quadratic regression (\clubsuit) provides a larger reduction in overhead of 51% with a normalised error of 0.626. This error is much larger error than that for the quadratic regression for the pressure conversion. Linear regression ($\color{orange}{\clubsuit}$) provides the best computational overhead with a reduction of 71% compared to the original but the normalised error is high at 4.77. Figure 3(c) shows that the RAM usage of the linear interpolation lookup table with 400 entries ($\color{green}{\star}$) is high, but the other methods on the Pareto frontier have lower resource usage than the original. If we exclude the linear interpolation lookup table with 400 entries ($\color{green}{\star}$), a smaller lookup table takes its place on the Pareto frontier. Most methods had larger error on the humidity conversion than on the pressure conversion. The linear interpolation lookup table with 400 entries ($\color{green}{\star}$) was an exception to this rule.

VI. RELATED WORK

As far as we are aware there is no prior work on using machine learning to find conversion routines with reduced computational overhead and memory requirements for an existing, commercially-available sensor. Two recent review papers discuss the use of machine learning for signal processing on the same physical hardware as the sensor but this requires bespoke hardware with integrated sensing and computing capability [8], [9]. Our method of learning new sensor

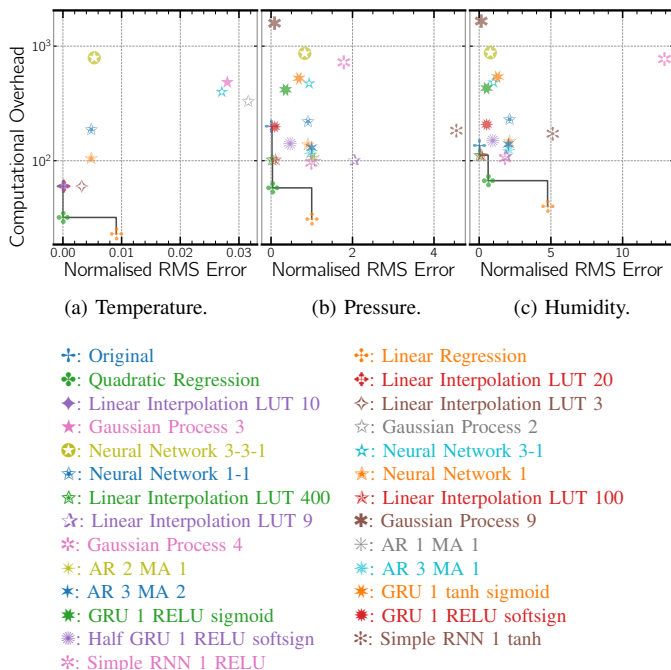


Fig. 2. Pareto plots for each conversion routine where smaller overhead and normalised RMS error is desirable. Pareto frontiers marked in black.

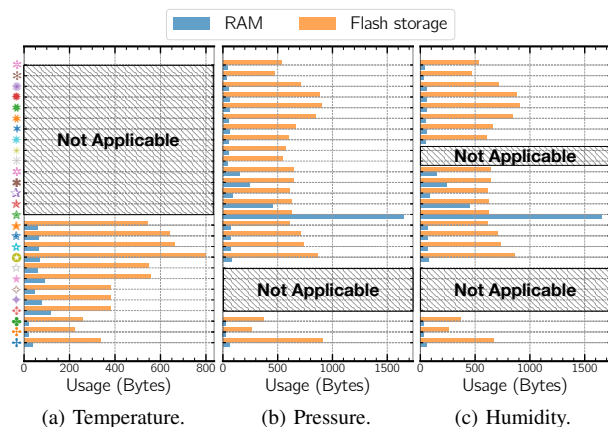


Fig. 3. RAM and flash storage usage of each model. The caption of Figure 2 shows the key for the y-axis. The hatched regions correspond to models which are not appropriate for the conversion routine being modeled or where we had prior knowledge that the quadratic regression would Pareto dominate all the sequence based methods.

conversion routines from data can run on existing hardware without modification. Oldfrey et al. present a machine learning approach that linearizes the output of cheap, highly-non-linear stretch sensors [7] and Zhang et al. reconstruct a full spectrum from reduced data [10]. Neither of these methods are directly applicable to the learning of sensor conversion routines for existing commercially-available sensors from data.

VII. CONCLUSION

Lookup tables with linear interpolation, quadratic regression, and linear regression are all superior to the original conversion routines in terms of computational overhead. The Pareto frontiers for all the conversions we tested were entirely occupied by function approximation methods: Sequence-based methods

ranging from ARMA to RNNs, LSTMs, and GRUs, were never on the Pareto frontier. The function approximation methods avoid the additional overheads of sequence models including initialising internal state, the possibility that error will be worse on some unusual sequences, and the possibility that some models may be unstable.

For temperature, linear regression provides a reduction in computational overhead of 62% with an error of 0.0114 C. For pressure, quadratic regression provides a 71% reduction in computational overhead and an error of 0.0280 kPa. For humidity, a linear interpolation lookup table with 400 data-points performs well with a 18% reduction in computational overhead and an error of 0.0337%.

Computational overhead reductions translate almost linearly to energy savings and are therefore useful in low-power systems using the BME680 sensor. There is no obvious reason why these methods will not work with similar sensors and their conversion routines.

ACKNOWLEDGMENTS

This research is supported by an Alan Turing Institute award TU/B/000096 under EPSRC grant EP/N510129/1, by EPSRC grant EP/V047507/1, and by the UKRI Materials Made Smarter Research Centre (EPSRC grant EP/V061798/1). The authors thank Vasileios Tsoutsouras and Orestis Kaparounakis for assistance with the figures.

REFERENCES

- [1] R. David, J. Duke, A. Jain, V. J. Reddi, N. Jeffries, J. Li, N. Kreeger, I. Nappier, M. Natraj, S. Regev *et al.*, “Tensorflow lite micro: Embedded machine learning on tinyml systems,” *arXiv preprint arXiv:2010.08678*, 2020.
- [2] *BME680 Datasheet*, Bosch Sensortec, <https://www.bosch-sensortec.com/media/boschsensortec/downloads/datasheets/bst-bme680-ds001.pdf>, 2020.
- [3] M. Abadi, A. Agarwal, P. Barham, E. Brevdo, Z. Chen, C. Citro, G. S. Corrado, A. Davis, J. Dean, M. Devin, S. Ghemawat, I. Goodfellow, A. Harp, G. Irving, M. Isard, Y. Jia, R. Jozefowicz, L. Kaiser, M. Kudlur, J. Levenberg, D. Mané, R. Monga, S. Moore, D. Murray, P. Olah, M. Schuster, J. Shlens, B. Steiner, I. Sutskever, K. Talwar, P. Tucker, V. Vanhoucke, V. Vasudevan, F. Viégas, O. Vinyals, P. Warden, M. Wattenberg, M. Wicke, Y. Yu, and X. Zheng, “TensorFlow: Large-scale machine learning on heterogeneous systems,” 2015, software available from tensorflow.org. [Online]. Available: <https://www.tensorflow.org/>
- [4] P. Stanley-Marbell and D. Marculescu, “Sunflower: Full-system, embedded, microarchitecture evaluation,” in *Proceedings of the 2nd International Conference on High Performance Embedded Architectures and Compilers*, ser. HiPEAC’07. Berlin, Heidelberg: Springer-Verlag, 2007, pp. 168–182.
- [5] C. E. Rasmussen, “Gaussian processes in machine learning,” in *Summer School on Machine Learning*. Springer, 2003, pp. 63–71.
- [6] J. Chung, C. Gulcehre, K. Cho, and Y. Bengio, “Empirical evaluation of gated recurrent neural networks on sequence modeling,” *arXiv preprint arXiv:1412.3555*, 2014.
- [7] B. Oldfrey, R. Jackson, P. Smitham, and M. Miodownik, “A deep learning approach to non-linearity in wearable stretch sensors,” *Frontiers in Robotics and AI*, vol. 6, p. 27, 2019.
- [8] F. Zhou and Y. Chai, “Near-sensor and in-sensor computing,” *Nature Electronics*, vol. 3, no. 11, pp. 664–671, 2020.
- [9] Z. Ballard, C. Brown, A. M. Madni, and A. Ozcan, “Machine learning and computation-enabled intelligent sensor design,” *Nature Machine Intelligence*, pp. 1–10, 2021.
- [10] S. Zhang, Y. Dong, H. Fu, S.-L. Huang, and L. Zhang, “A spectral reconstruction algorithm of miniature spectrometer based on sparse optimization and dictionary learning,” *Sensors*, vol. 18, no. 2, p. 644, 2018.